

# Abelian Sandpiles on Cylinders

Jean-Pierre Eckmann<sup>1,2</sup>, Tatiana Nagnibeda<sup>2</sup>, Aymeric Perriard<sup>1</sup>

<sup>1</sup> Département de Physique Théorique. University of Geneva, Switzerland

<sup>2</sup> Section de Mathématiques. University of Geneva, Switzerland

**Abstract.** We study the Abelian Sandpile Model on a special playground, a cylinder of width  $w$  and of circumference  $c$ . When  $c \ll w$ , we describe a phenomenon which has not been observed in other geometries: the probability distribution of avalanche sizes has a ladder structure, with the first step consisting of avalanches of size up to  $w \cdot c/2$  that are essentially equiprobable, except for a small exponential tail of order about  $10c$ . We explain this phenomenon and describe subsequent steps.

*Keywords:* Abelian sandpile models, cylinder, random walk

Submitted to: *J. Phys. A: Math. Theor.*

## 1. Introduction

Abelian sandpile models (ASM) come in many guises. Such a model is usually based on a lattice or, more generally, on a connected graph of bounded degree and describes the dynamics of sandpiles on the nodes of the graph. It obeys the following evolution rule: if there are at least  $n$  grains of sand on a node with  $n$  neighbors, then the node "topples," which means that one grain of sand is moved from this node to each of its  $n$  neighbors. It is usually assumed that the system has some dissipative nodes which guarantee that every configuration of sandpiles stabilizes eventually. The beauty of the ASM is that the resulting stable configuration is independent of the order in which unstable nodes were toppled (Dhar 1990). The sequence of topplings in the process of stabilizing an unstable configuration is called an avalanche. ASM has been invented by (Bak et al. 1987) to understand the phenomenon of self-organized criticality (SOC) with emphasis on the power law behavior of the avalanche distribution.

The ASM on the regular square lattice has been abundantly studied. The 1-dimensional case can be solved exactly and has been proven to be non-critical (Dhar & Majumdar 1990) in the sense that the number of avalanches of size  $s$  decreases exponentially in  $s$ . In the 2-dimensional case one approximates the lattice  $\mathbb{Z}^2$  by finite squares  $\Lambda_n$  with growing size  $n$ . New grains of sand are added uniformly in  $\Lambda$  to re-initiate the avalanches. If grains leave  $\Lambda$ , they are lost, and this makes the process dissipative. Various measurements of the avalanches and other correlation functions have been introduced to prove criticality of the model, but it seems that in most cases there is no consensus on the exact power law that they obey (see e.g., (Manna 1991, Priezzhev et al. 1996)). Besides throwing new grains of sand into the system uniformly at random, another popular choice is to add new grains of sand always at the same fixed position. One then observes beautiful symmetric patterns which form as more and more grains are added (Levine & Propp 2010).

The purpose of our work is to interpolate between the models in 1D and 2D by considering the ASM on discrete cylinders of width  $w$  (preferentially an odd integer) and circumference  $c \geq 2$  with dissipative boundary, as shown in figure 1.

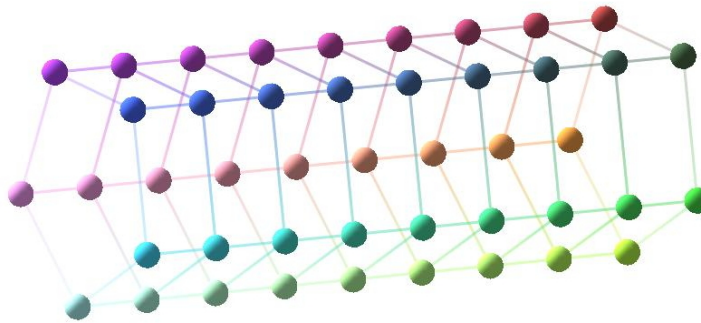


**Figure 1.** A cylinder of width  $w = 9$  and circumference  $c = 5$ . Grains can only fall off at the two ends of the cylinder.

Regarding the rule according to which the avalanches are reinitialized, we study yet another variant which interpolates between the two extreme scenarios described above: the

grains are added uniformly at random but only near the center of the cylinder, for example, uniformly among the nodes with horizontal coordinate  $x = w/2 \pm 1$  and  $w/2$  (with  $w$  even). We measure the size of avalanches, *i.e.*, the number of topplings that form an avalanche.

We will study these models for  $w$  large, and  $c$  small, and will explain the behavior in a limit of  $w \rightarrow \infty$ , for fixed  $c \geq 2$ . We will also make some remarks on what happens as  $c$  grows and becomes comparable to  $w$ .

Our numerical studies show a behavior which seems novel in this context, see figure 2. Namely, the distribution of avalanche sizes, for avalanches of medium size, shows distinct plateaus (steps) of equiprobable avalanche sizes, which somehow contrasts the idea of power law decay (it does appear for relatively small avalanches, and for  $c \sim w$ , as discussed in figure 8 later on). A similar behavior was observed in (Daerden & Vanderzande 1998) who studied the ASM on a Sierpinski gasket; in this case, the plateaus are connected with the hierarchical structure of the gasket.

Our main result is an explanation of why these unexpected plateaus appear, that is, why a large range of avalanche sizes are basically *equiprobable*. The main observation is that the position of the end of the avalanche (farthest from the center of the cylinder) performs a *random walk*. When projected onto  $\mathbb{Z}$ , such random walks visit the sites between the center and the ends of the cylinder with uniform probability, as is well-known (Spitzer 1964, “Random Walk on an Interval”, pp. 247–273). Therefore, all sizes of avalanches are seen to be equiprobable (in the range  $0, \dots, w/2 \cdot c$ ). We will also explain the second and third plateaus in a similar vein.

## 2. Detailed arguments

In our model, we are interested in the statistics of the avalanche sizes as a function of the width  $w$  and of the circumference  $c$  of the cylinder. Obviously, if the node on which the new grain is dropped has  $\leq 3$  grains, no toppling happens and no avalanche is formed: we say that the avalanche has size 0. This happens about 50% of the time.

Inspection of the data shows that, except near the center of the cylinder, most sites have actually 3 grains (are filled). When a grain arrives, say, from the left on a horizontal position  $x \in \{\lceil w/2 \rceil, \dots, w\}$ , if all  $c$  sites in the  $x$  position are filled, they will all topple once, and propagate the front of the avalanche to the right.

For each  $x \in \{1, \dots, w\}$  we compute  $s(x) = \sum_{y=1}^c n(x, y)$ , where  $n(x, y)$  is the number of grains at the node  $(x, y)$ . If  $s(x) < 3c$  then we say that  $x$  is a *blocker*. If there is no blocker inside the cylinder on a given side from the center, then we say that the boundary of the cylinder is a blocker (*i.e.*,  $x = 1$  or  $x = w$ ).

We start by summarizing the numerical observations, and then we will explain their mathematical origins.

We first note, as shown in figure 6, that there are two salient features of the model. There is, at any given time, (*i.e.*, after the system comes to rest when one grain has been added) exactly 1 blocker, either on the left or on the right of the center of the cylinder (we neglect here a

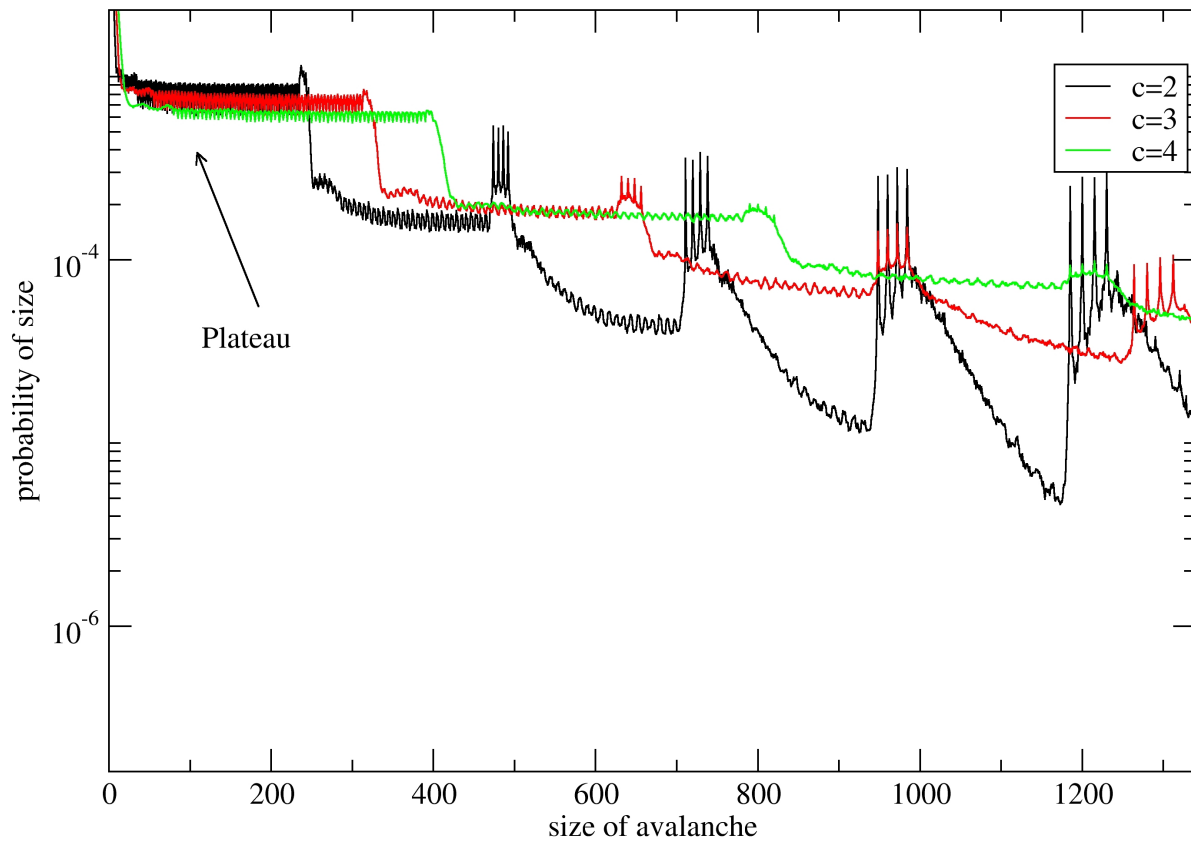


**Figure 2.** The probability of an avalanche of size  $x$  for cylinders of width  $w = 160$  and circumferences  $c = 3, 4$ , and  $5$ . The first plateaus have size about  $w \cdot c/2$ . The data were acquired by adding  $2 \cdot 10^8$  grains (for each fixed  $c$ ). About half of the events produce no avalanche.

region of size about  $c$  in the  $x$ -direction near the center where more grains may be missing). After each avalanche, the blocker either moves by at most  $\pm 1$  in the  $x$ -direction, or jumps to the other side of the cylinder with respect to the center. Inspection of the figure suggests that the distance between the blockers is close to  $w/2$ , as is seen by the symmetries in the vertical direction. Furthermore, the position of the blocker, as a function of the avalanche count, looks like a random walk in the  $x$ -direction.

Recall that once the system has reached a stable (recurrent) configuration the dynamics is reinitialized by adding a new grain randomly in the central part of the cylinder. An avalanche is a multiset of nodes that become unstable as a result, and we are interested in its size. These unstable nodes can be toppled in any order resulting in the same new recurrent configuration. As in (Prietzhev et al. 1996, Dhar 2006), an avalanche is partitioned into “waves” in which each node topples at most once. When examining avalanches on a cylinder, we find it useful to choose moreover a specific order in which the unstable nodes will be toppled. Namely, we perform “swipes” which consist in running the cylinder from left to right (or from right to left) and toppling the nodes that are unstable. By the Abelian property, the stable configuration in which the avalanche results is independent of the order of topplings and in particular of the direction in which the swipe is performed.

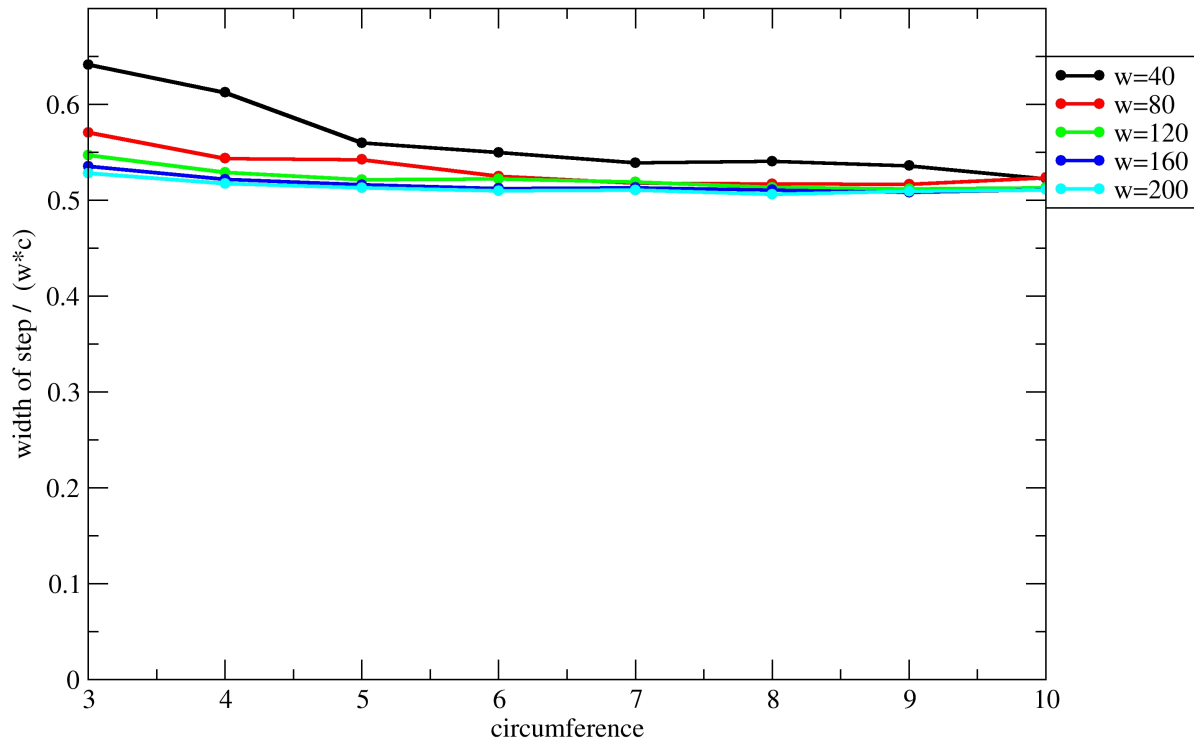


**Figure 3.** The width of the (first) plateau, divided by  $w \cdot c$  for  $w = 40, 80, \dots, 200$ , and  $c = 3, \dots, 10$ . The convergence to 0.5 is manifest.

This allows us to analyze the nature of avalanches in the first 3 plateaus in figure 4, and we see that the avalanche formation is of different qualitative nature: In the first plateau, at each swipe, there are 2 topplings, in the second, 5, and in the third up to 10. These topplings form the advancing front of the avalanche until it reaches a blocker. The front becomes wider as we move to avalanches in the next plateau.

In figure 7 we illustrate the detailed fillings near the horizontal center of the cylinder. Here, it is visible that there are several sites which are not fully occupied, and bigger holes are the initiators of larger avalanches.

We also check, in figure 3 the width of the first plateau (as a function of  $w$  and  $c$ ) is basically  $w \cdot c/2$ .

With these illustrations at hand, we can now prove the existence of the first plateau. Let  $x$  denote the distance between the center of the cylinder and the right blocker. Because the blocker performs a random walk, the density probability function  $\varrho(x)$  is constant in the interval  $d \in (0, w/2)$ .

When the right blocker is at a horizontal position  $x$  and a single front avalanche moves to the right, its size  $s$  is equal to  $c \cdot x$  (up to some neglected initial topplings in the center).

Thus the probability density function  $\varrho(s)$  of the single right-moving avalanches is constant, going from  $s = 0$  to  $s = wc/2$  (the biggest avalanche corresponds to  $x = w/2$ ). By symmetry, the case for the left blocker is the same, and thus  $\varrho(s)$  is independent of  $s$ . This

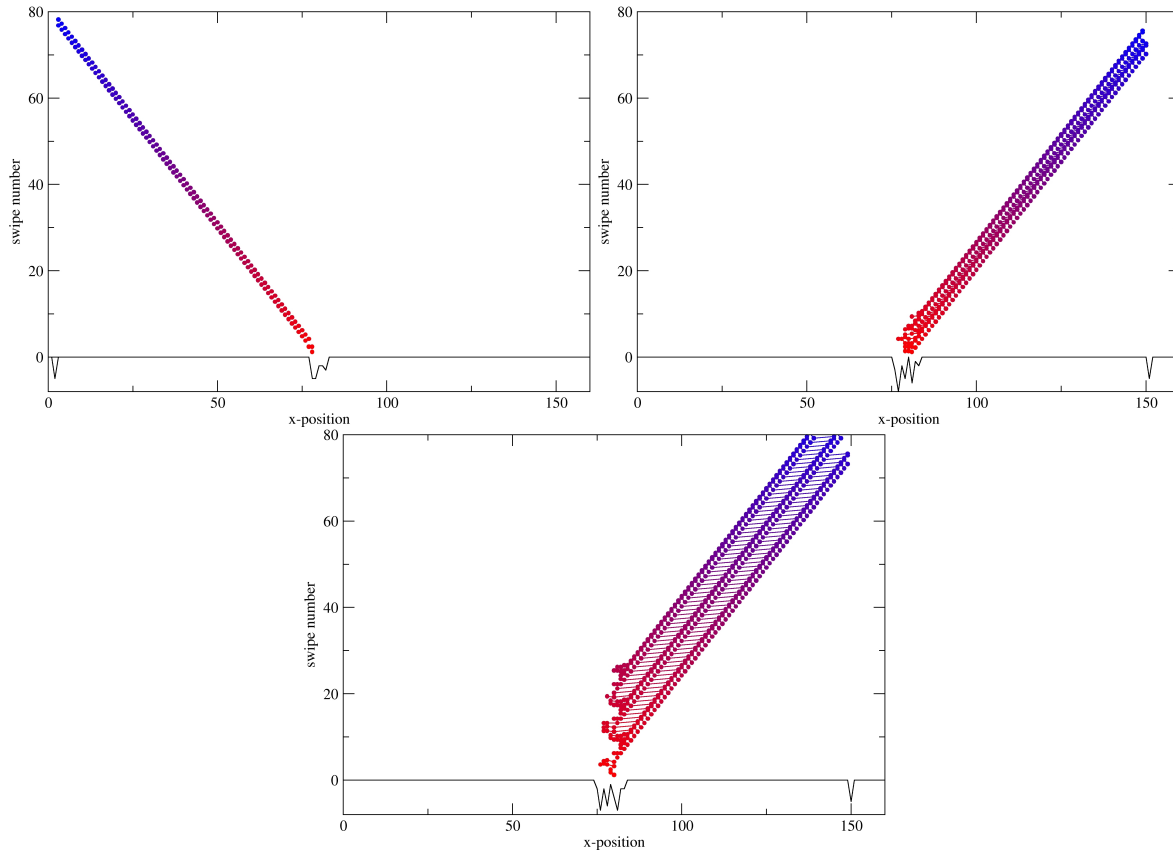


**Figure 4.** The geometry of a typical avalanche from plateau 1 (top left), 2 (top right), and 3 (bottom). In these samples,  $w = 160$  and  $c = 5$ . The avalanches have sizes 1516, 2880, and 4300, for the cases of plateau 1, 2, and 3 shown in the 3 panels. The horizontal axis is the  $x$  position from 0 to  $w$ , the vertical axis is the time steps of the toppling algorithm. These figures illustrate that larger avalanches are created by wider fronts (respectively, single, double and triple for the three panels). These wider fronts occur whenever the random motion in the center creates a big enough set of non-filled positions (as shown by the black line). These black lines at the bottom indicate the filling of the cylinder with the line at height 0 corresponding to all  $c$  sites at fixed  $x$  having 3 grains.

corresponds to the first plateau we observe.

### 3. Behavior of small avalanches for varying $c$

We did extensive experiments, with up to  $10^8$  rounds of throwing sand, to check the power law behavior, for fixed  $w = 160$  and varying  $c$ . The data are sampled logarithmically. Numerical verification shows that for sizes  $c = 120$  and  $c = 160$ , the decay corresponds to a power law  $n^{-\alpha}$ , with  $\alpha \sim 1.035$ , see figure 8. Note also that in this figure, the incipient plateaus are visible for small  $c$  and become less and less pronounced as  $c$  increases.

Furthermore, one can consider the avalanches with size between  $10c$  and  $w \cdot c/2$ , i.e., the avalanches forming the first plateau. There are  $n = w \cdot c/2 - 10c$  possible sizes  $s$  of the avalanches, and each one appears empirically  $n(s)$  times when we do  $N$  avalanches. We

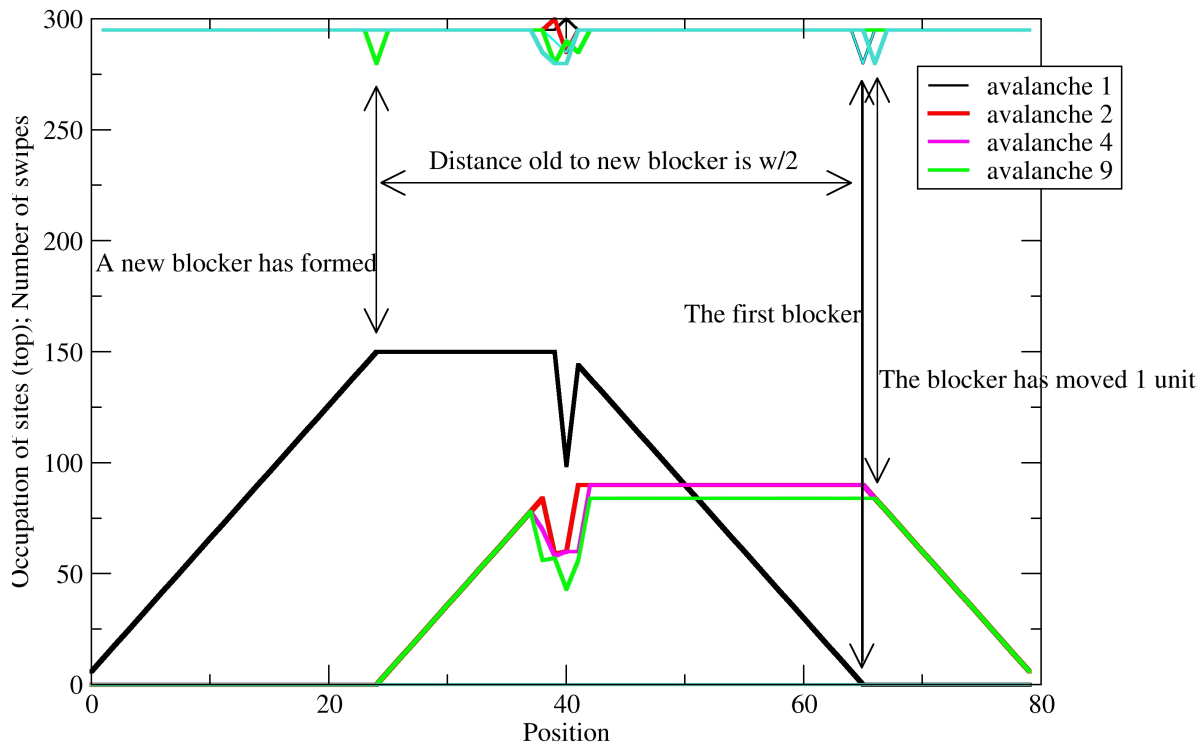


**Figure 5.** An illustration of how blockers move. The simulation starts with a full cylinder  $w = 80$ ,  $c = 3$  except with one grain of sand missing at position 65. We examine several avalanches (others were short, just around position  $40 = w/2$ ) that occur when adding one grain to this configuration according to our rules. The first avalanche (in black) needs an increasing number of swipes as a function of the distance from 65 and from 0 (the number of the swipe in which the given site will be toppled grows). A new blocker is created near position 25. In the ninth avalanche (green) the number of the swipes is growing from that position and this entails the move of the first blocker one unit to the right. This is how the random walk is generated.

define

$$P(x)dx = \text{number of } s \text{ for which } n(s)/N \in [x, x + dx] .$$

One expects  $P(x)$  to be constant, but there are fluctuations: Upon about  $N \sim 10^6$  topplings for  $w = 4000$  and  $c = 3$ , we see that  $\log(P(x))$  is close to a quadratic function, which means that the empirical distribution of  $P(n)$  is Gaussian, see figure 9. This indicates that the *variations* of the toppling sizes within the plateau are independent.

#### 4. The case $c = 1$

It is of course tempting to consider separately the case  $c = 1$  and to compare it with the 1-dimensional sandpile models that have appeared in the literature, notably with (Ali & Dhar 1995a, Ali & Dhar 1995b) where certain decorated chains are studied in great detail.

In our model, for the case  $c = 1$ , the cylinder is reduced to a chain with a loop attached at each position  $x \in [1, \dots, w]$ , and the rule we apply is that if there are 3 grains at a site  $x$  and

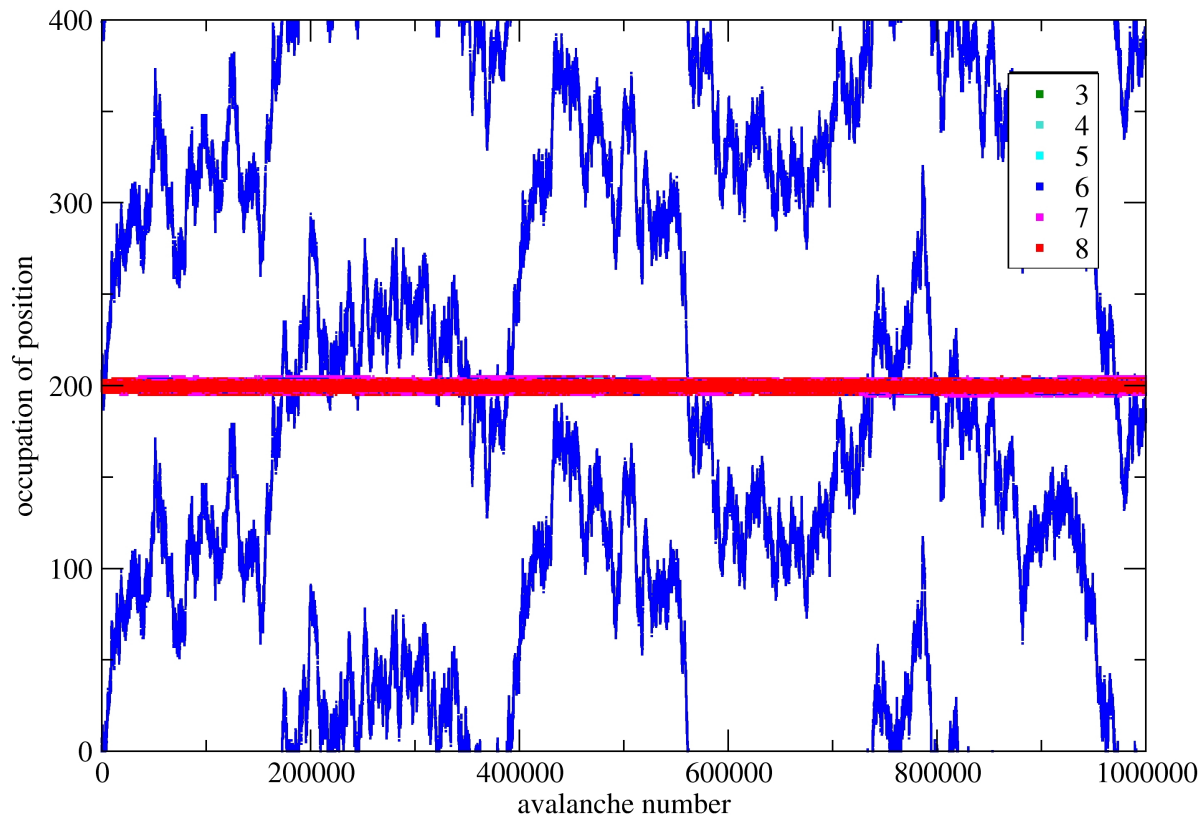


**Figure 6.** An illustration of the motion of the blockers (for the first million avalanches) when  $w = 400$  and  $c = 3$ . The positions of the blocker (coloured in blue) form a trajectory of a random walk. Furthermore, the distance between the blockers in the top and bottom half of the cylinder (the vertical axis) is always very close to  $w/2$ . The blockers (the blue points) always have 6 of the maximal possible number of grains which is  $9 = 3c$ . (Actually, 1 grain is missing for every point on the cylinder with fixed  $x$ .) The red horizontal band near the center, around position 200, is better resolved in figure 7 where one also better sees points near the center colored in other colors according to the number of grains (see the color code). Note that "full" sites (with 9 grains) are left white.

one grain arrives to it, the site topples, sending two grains "around" the loop, and one grain to the left and the right, respectively. In their case, the decorations are either a double link from node  $2n$  to  $2n + 1$  with  $n \in \mathbb{Z}$  or a losange inserted at each second node. The new grains are added randomly and uniformly on every site. A careful analysis of possible avalanche types leads to asymptotic formulas for the avalanche length distribution (in  $w$  (their  $L$ )). In our model we add sand randomly uniformly only to the positions adjacent to the center of the cylinder or to the central positions. In this case, the avalanches are uniformly distributed over all possible lengths, as can be verified numerically. If one fits a straight, horizontal line, the standard error is seen to decrease with the size of the system. A analytic proof seems possible, but is out of the scope of this paper.



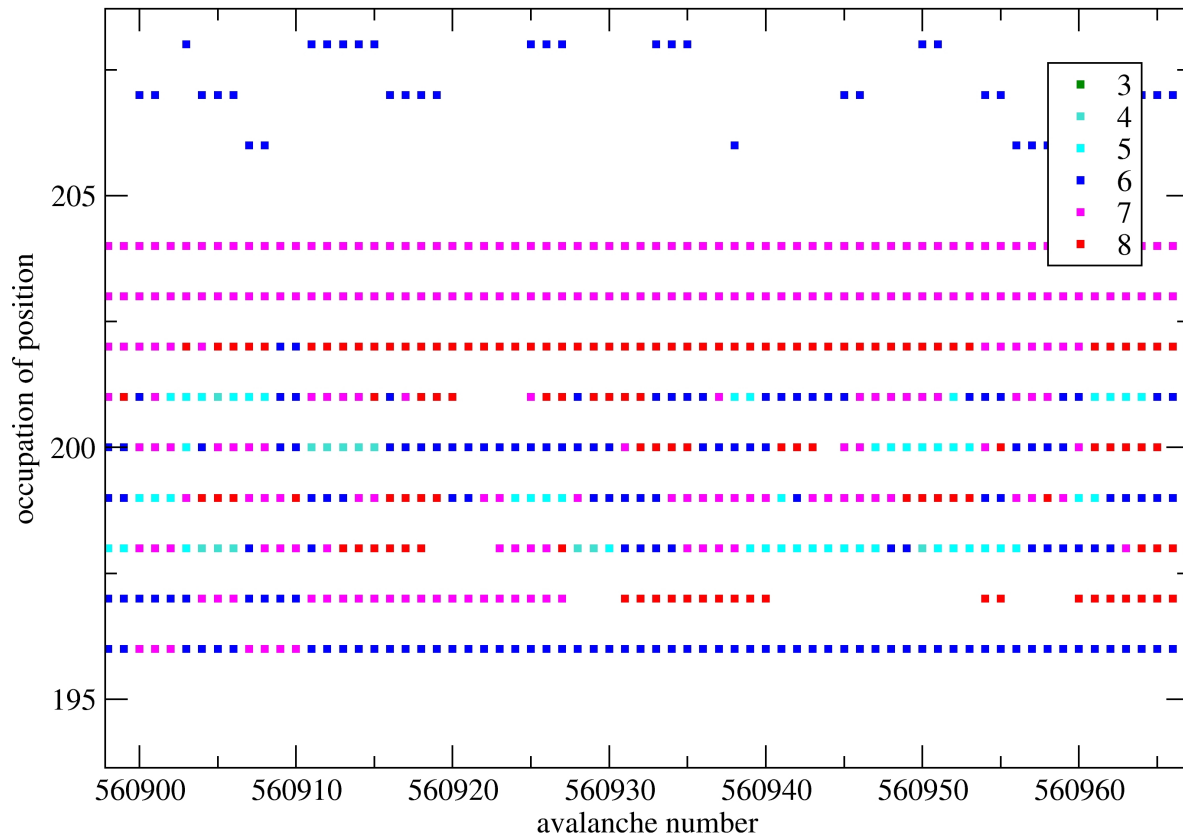


**Figure 7.** A magnification of the center of figure 6: The red horizontal band near the center is now resolved into a band with a variety of occupation numbers, between 3 and 8, which covers avalanches around 560000 and positions between 194 and 208. Note that "full" sites (with 9 grains) are left white.

## 5. $1/f$ behavior

Upon suggestion by Ramakrishna Rawaswamy, we also checked the  $1/f$  behavior of the filling of the cylinder. The cylinder can have a maximum of  $3w \cdot c$  grains of sand at each site in a stable configuration. We have checked the temporal distribution of the number  $n(t)$  of grains in the cylinder after the injection of  $t$  grains of sand. We take the Fourier transform of these numbers (normalized to mean 0) and plot the result in figure 10. The linear fit shows that the power as function of the frequency  $f$  behaves like  $1/f^\alpha$  for a positive  $\alpha$  ( $\alpha$  depends on the scale of  $t$  we take).

## 6. Correlations between the process of throwing sand and the motion of the blockers.

We have compared our results with the case when the horizontal position where new grains are added is fixed exactly at the center of the cylinder (as opposed to it being chosen randomly over a small neighborhood of the central position as in the previous sections). The avalanche distribution is not the same and we do not observe a random walk of the blocker.

If the position where the new grains fall is fixed but not at the center, for example, if  $w$

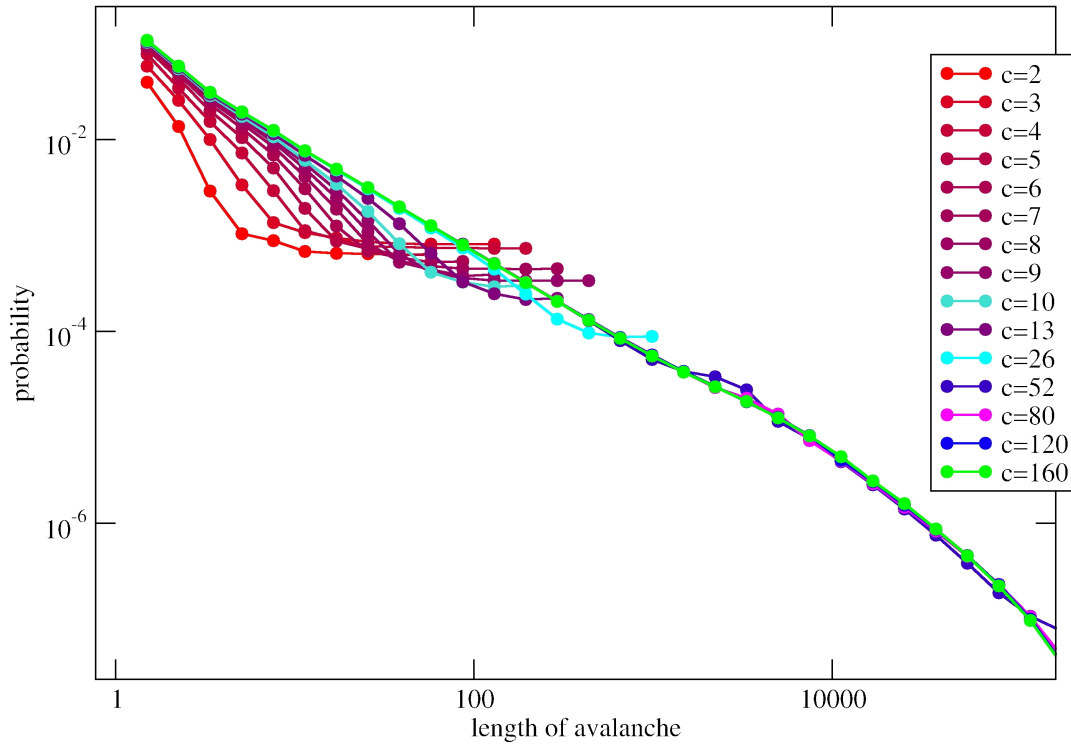


**Figure 8.** Power law behavior for small avalanches, for the case  $w = 160$  and several  $c$ . This is the left end of figure 2, but now the  $x$ -axis is logarithmic. Note that the power law depends on  $c$  (for fixed  $w$ ) and reaches  $\sim 1.035$  when  $c = 160$ . For small  $c$  we see the incipents of the first plateau. To make the figure less crowded, for each  $c$  we stop drawing the curves once the plateau is reached (the first point where the numerical derivative is positive). The curves are obtained from about  $0.85 \cdot 10^9$  avalanches.

is even, and the grain falls at  $(w - 1)/2$ , the behavior is as in the random case, except that the blocker just moves linearly to positions with lower  $x$ -coordinates. Therefore, plateaus are visible as in the random case we studied above. This suggests that there might be a correlation between the direction of the move of the blocker and the side at which the grain is randomly thrown, say, at  $(w - 1) \pm 1$  when  $w$  is odd.

In figure 11 we illustrate the random walk for an example with  $w = 101$  and  $c = 6$ . While the illustrated data have a Pearson coefficient of 0.77, on longer runs there are less good correlations, because there are additional phase shifts between the two curves. (The symmetries visible in figure 6 have been taken into account by mapping all events to the interval  $1 \leq x \leq w/2$ .)

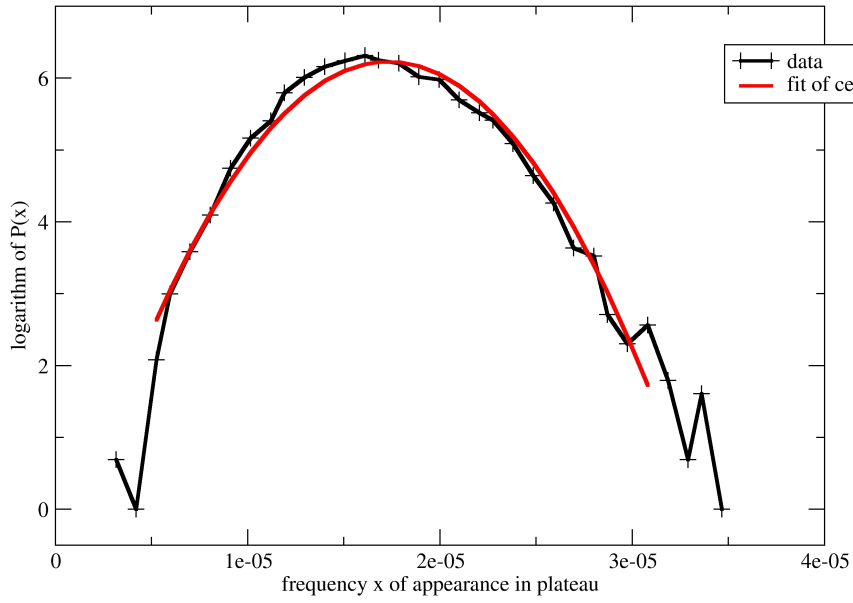


**Figure 9.** A numerical verification of the Gaussian fit for  $w = 4000$  and  $c = 3$ , for  $10^6$  topplings. This makes for a very wide plateau, and we sample the number of times each size of the avalanche occurs. This is seen to be a Gaussian distribution.

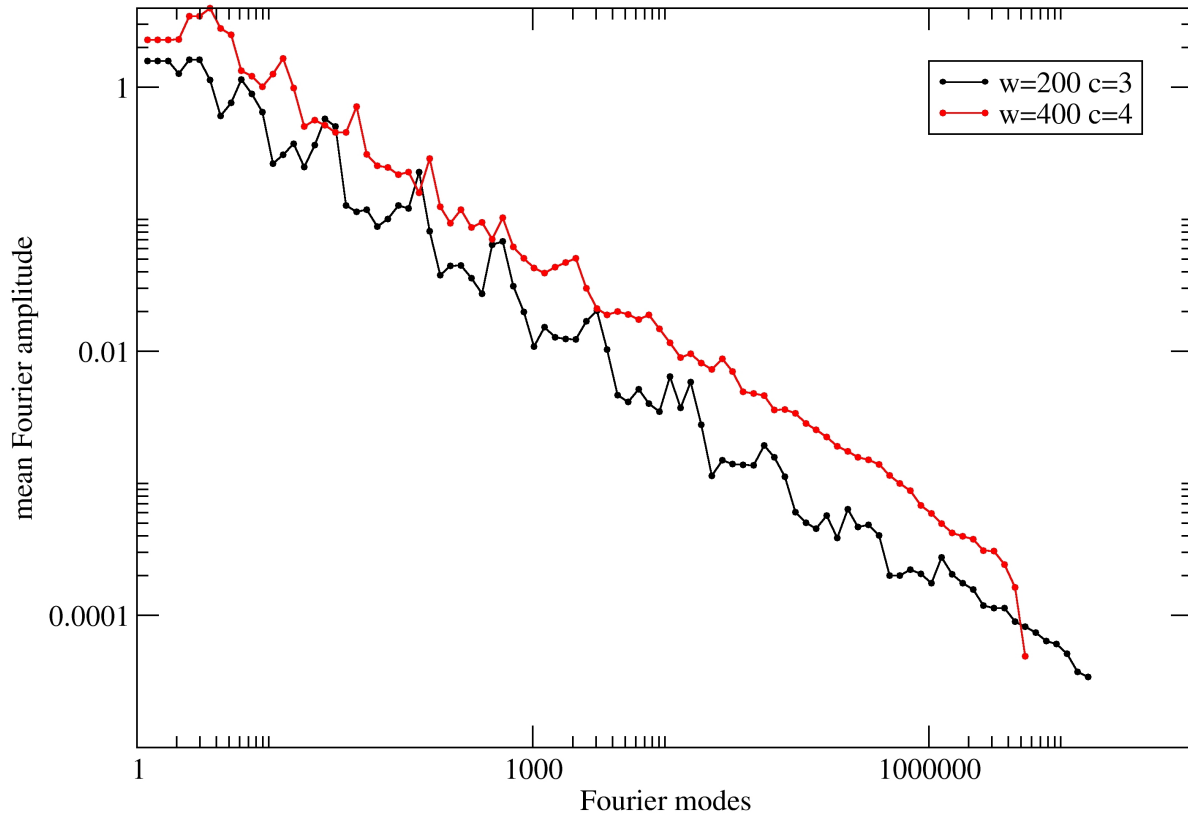


**Figure 10.** Let  $n(t)$  be the total number of grains in the cylinder after  $t$  grains have been thrown. We show the Fourier transform of  $n(t)$  for two values of  $w$  and  $c$ . The graph clearly shows a power law (the same in both cases). The number of samples is  $\sim 16 \cdot 10^6$  for cylinder width  $w = 200$  and  $\sim 5 \cdot 10^6$  for  $w = 400$ .

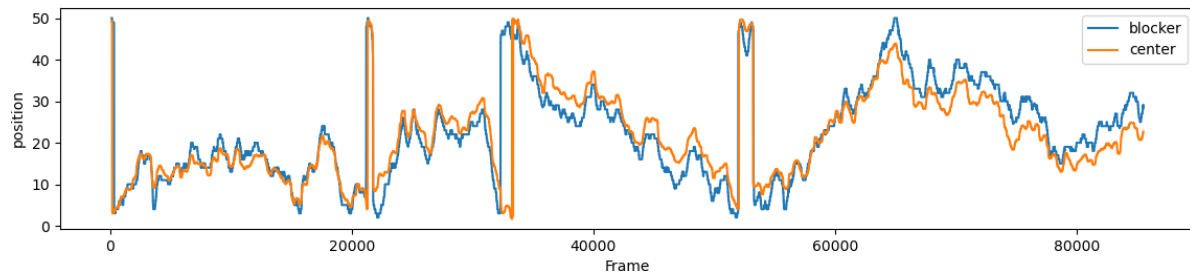


**Figure 11.** Correlation between the random walk generated by the  $\pm 1$  choices of where the grain is thrown (orange) and the position of the blocker (blue); sliding average over 300 data points.

## Acknowledgments

JPE is partially supported by Swissmap. TN acknowledges support of the FNS grant 200020-200400.

## References

- Ali A A & Dhar D 1995a *Phys. Rev. E* **51**, R2705–R2708.  
**URL:** <https://link.aps.org/doi/10.1103/PhysRevE.51.R2705>
- Ali A A & Dhar D 1995b *Phys. Rev. E* **52**, 4804–4816.  
**URL:** <https://link.aps.org/doi/10.1103/PhysRevE.52.4804>
- Bak P, Tang C & Wiesenfeld K 1987 *Phys. Rev. Lett.* **59**, 381–384.  
**URL:** <https://link.aps.org/doi/10.1103/PhysRevLett.59.381>
- Daerden F & Vanderzande C 1998 *Physica A: Statistical Mechanics and its Applications* **256**(3-4), 533–546.  
**URL:** [https://doi.org/10.1016/s0378-4371\(98\)00210-6](https://doi.org/10.1016/s0378-4371(98)00210-6)
- Dhar D 1990 *Phys. Rev. Lett.* **64**, 1613–1616.  
**URL:** <https://link.aps.org/doi/10.1103/PhysRevLett.64.1613>
- Dhar D 2006 *Physica A* **369**, 29–70.  
**URL:** <https://doi.org/10.1016/j.physa.2006.04.004>
- Dhar D & Majumdar S N 1990 *Journal of Physics A: Mathematical and General* **23**(19), 4333.  
**URL:** <https://dx.doi.org/10.1088/0305-4470/23/19/018>
- Levine L & Propp J 2010 *Notices Amer. Math. Soc.* **57**(8), 976–979.
- Manna S 1991 *Physica A: Statistical Mechanics and its Applications* pp. 249–268.
- Priezzhev V, Kitzrev D & Ivashkevich E 1996 *Phys. Review Letters* **76**(12), 2093–2097.
- Spitzer F 1964 *Principles of Random Walk* Springer New York New York, NY.